

Supporting information

**An advanced composite with ultrafast photocatalytic performance for
degradation of antibiotics by natural sunlight without oxidizing source over
TMU-5@Ni-Ti LDH: Mechanism insight and toxicity assessment**

Reza Abazari,^a Ali Morsali,^{a*} and Deepak P. Dubal^b

^a*Department of Chemistry, Tarbiat Modares University, P.O. Box 14115-175, Tehran, Iran*

^b*School of Chemistry, Physics and Mechanical Engineering, Queensland University of Technology
(QUT), 2 George Street, Brisbane, QLD 4001, Australia*

**E-mail: morsali_a@modares.ac.ir*

Physical techniques

The morphology of samples was characterized by field emission scanning electron microscope (FE-SEM) Hitachi S-1460 with gold coating. The infrared spectra were recorded on Nicolet Fourier transform IR, Nicolet 100 spectrometer in the range of 400-4000 cm^{-1} using KBr pellets. Surface area, pore diameter and total volume of samples were calculated according to Brunauer-Emmett-Teller (BET) method by TriStar 3020 (Micromeritics instrument corp.) analyzer. The UV-Vis absorption spectra were examined on a 4802 UV-Vis spectrometer Unico in the wavelength range of 200-800 nm. PXRD patterns were carried on STOE power diffraction system at 40 kV and 40 mA equipped with a $\text{Cu}/\text{K}\alpha$ ($\lambda=1.54060 \text{ \AA}$) radiation source. XRD spectra were recorded in a 2θ range of 1-80°. UV-Vis diffuse reflectance spectra (DRS) was measured by Shimadzu-UV-2550-8030 spectrophotometer in the range of 200-800 nm with slit width of 5.0 nm and light source with wavelength of 360 nm at room temperature. Barium sulfate (BaSO_4) was applied as reflectance standard. To perform the electrochemical tests, the Bio-Logic SP-300 was used. The inductively coupled plasma (ICP) analysis was performed on a Varian ICP-OES VISTA-PRO CCD instrument. Ultrasonic generators were carried out on a SONICA-2200 EP, input: 40-60 kHz/305W.

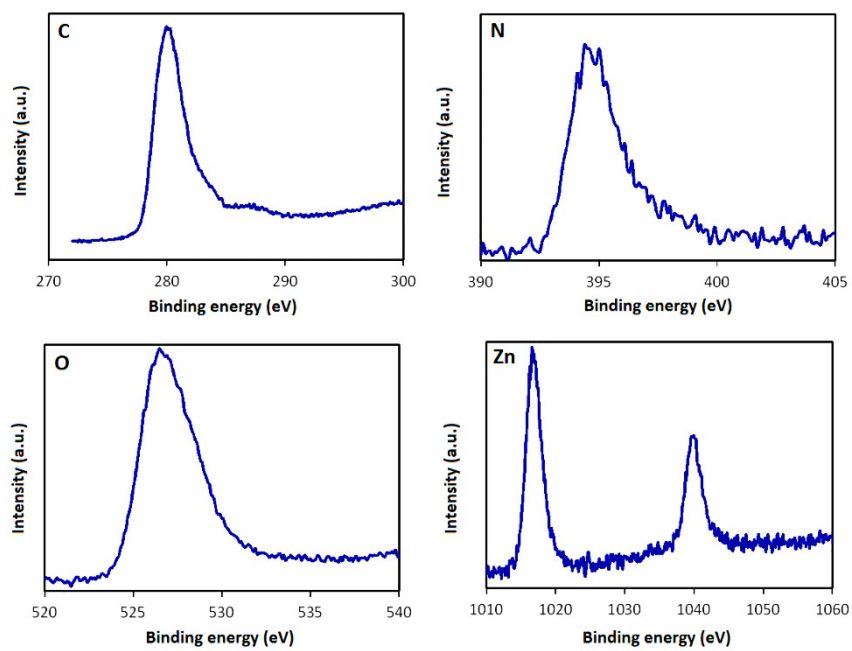


Figure S1. The XPS spectra of the pure Zn-TMU-5.

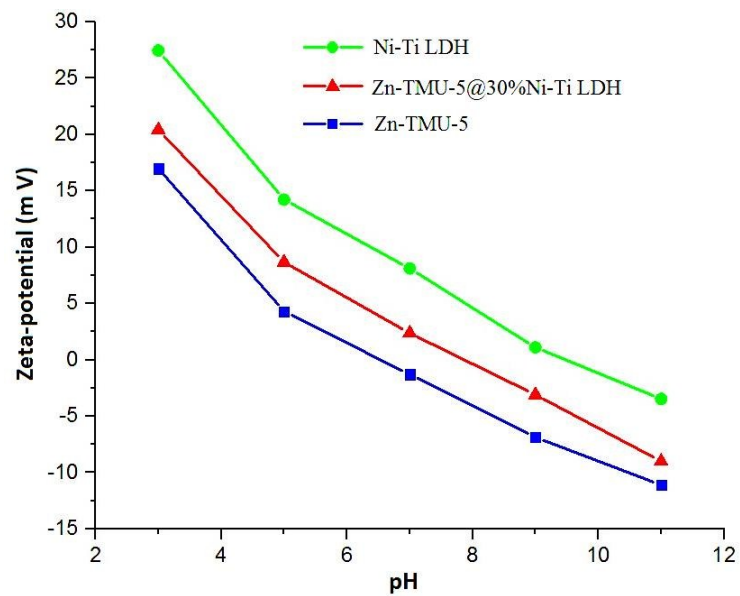


Figure S2. Effect of pH on the zeta potential of Ni-Ti LDH, Zn-TMU-5 and Zn-TMU-5@30%Ni-Ti LDH.

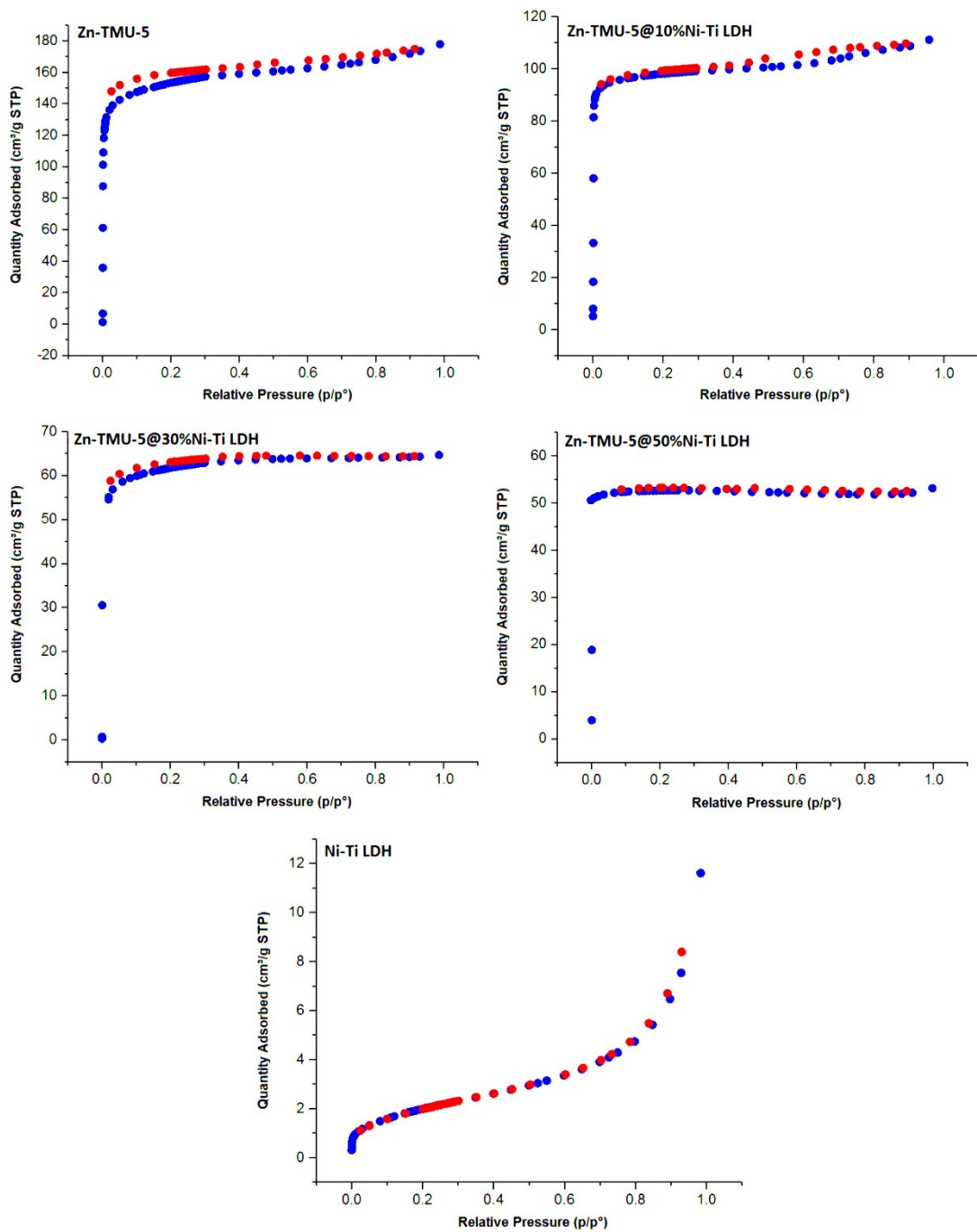


Figure S3. The nitrogen adsorption-desorption isotherms of Ni-Ti LDH, Zn-TMU-5 and Zn-TMU-5@X%Ni-Ti LDH.

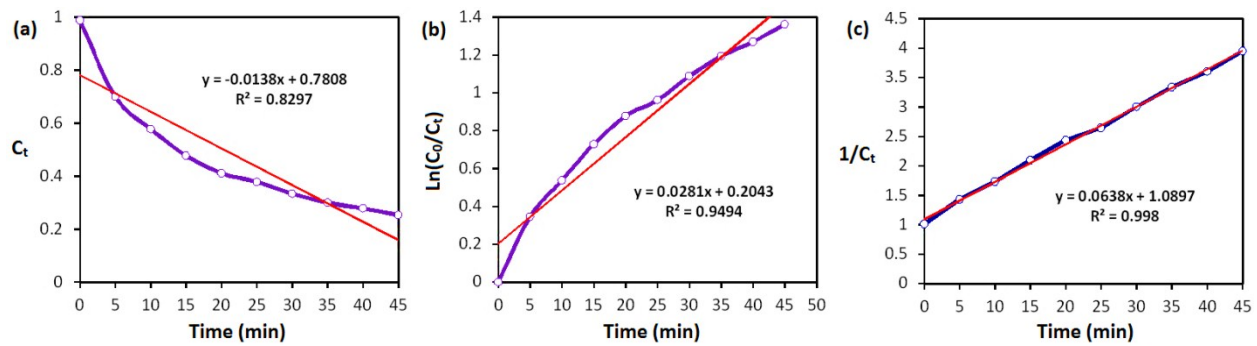


Figure S4. Reaction kinetics of SMZ degradation over Zn-TMU-5@30%Ni-Ti LDH composites: (a) zero (b) first and (c) second order.

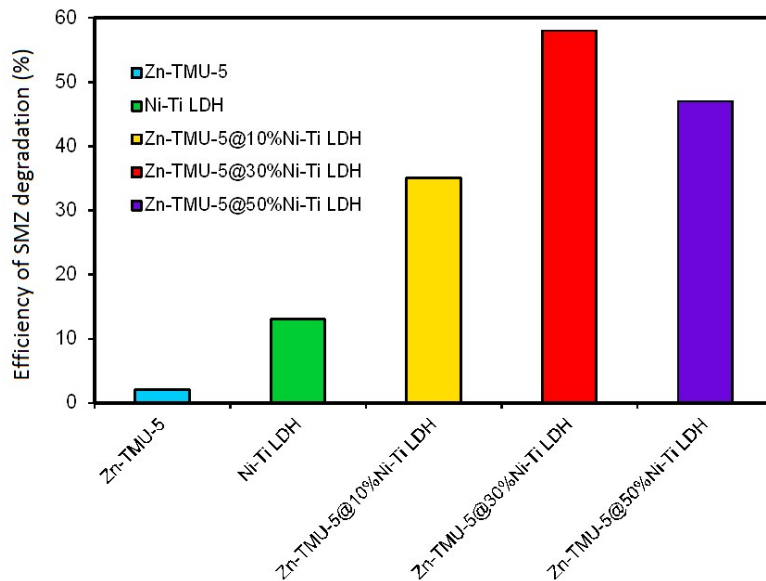


Figure S5. TOC removal efficiency of SMZ by Ni-Ti LDH, Zn-TMU-5 and Zn-TMU-5@X%Ni-Ti LDH after 45 min under sun light irradiation.

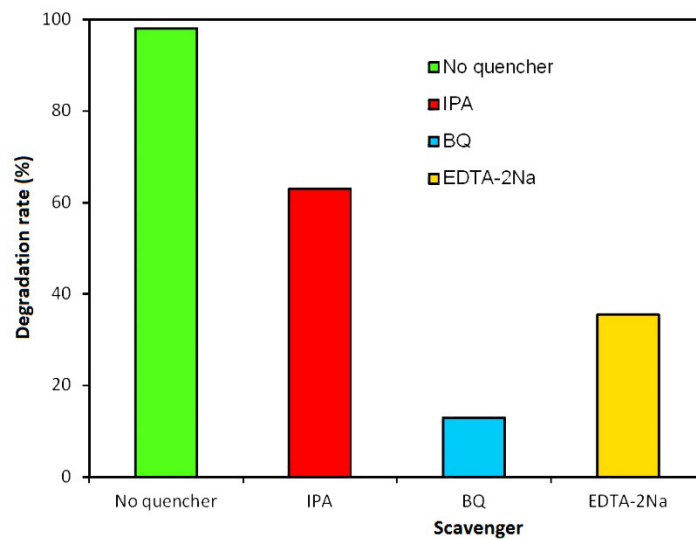


Figure S6. Effects of various active scavengers on the degradation of SMZ over Zn-TMU-5@30%Ni-Ti LDH composites under natural solar light irradiation after 45 min.

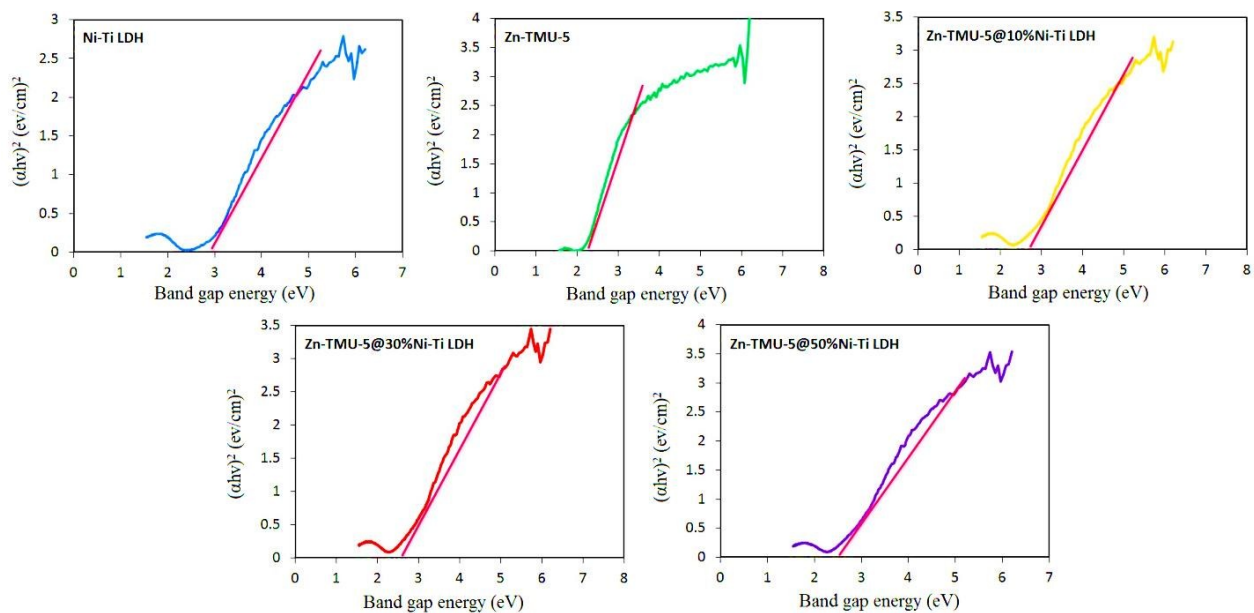


Figure S7. Specific absorption band edges calculated using the Tauc relationship of Ni-Ti LDH,

Zn-TMU-5 and Zn-TMU-5@X%Ni-Ti LDH.

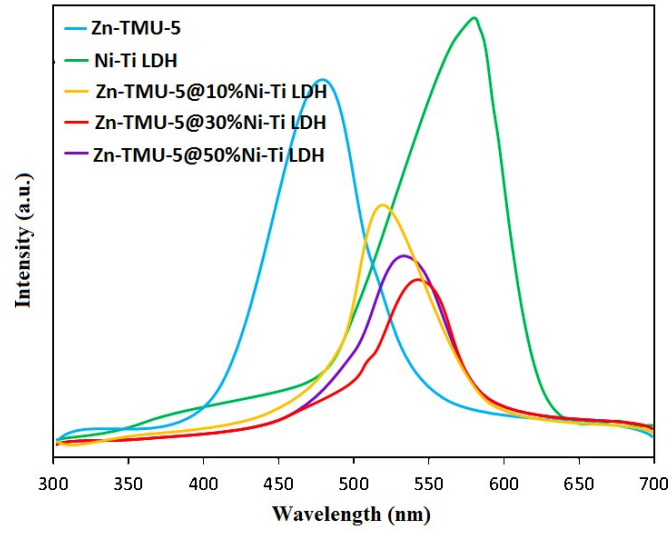


Figure S8. The PL spectra of Ni-Ti LDH, Zn-TMU-5 and Zn-TMU-5@X%Ni-Ti LDH composites.

Table S1. Binding energy (eV) of Zn-TMU-5 and Zn-TMU-5@X%Ni-Ti LDH.

Binding energy (eV)	Zn	Ni	Ti	C	N	O
Zn-TMU-5	1018.4 (Zn 2p3/2) and 1042.7 (Zn 2p1/2)	-	-	281.9 (C1s)	397.6 (N1s)	526.7(O1s)
Zn-TMU-5@X%Ni-Ti LDH	1017 (Zn 2p3/2) and 1041 (Zn 2p1/2)	854 (Ni 2p3/2) and 870 eV (Ni 2p1/2)	455 (Ti 2p1/2)	280.6 (C1s)	396 (N1s)	525.1 (O1s)

Table S2. ICP analysis of Ni-Ti LDH, Zn-TMU-5 and Zn-TMU-5@X%Ni-Ti LDH.

Wt.%	Zn-TMU-5	Ni-Ti LDH	Zn-TMU-5@10%Ni-Ti LDH	Zn-TMU-5@30%Ni-Ti LDH	Zn-TMU-5@50%Ni-Ti LDH
Zn	100	0	84	65	46
Ni	0	72	11.50	25	40
Ti	0	28	4.50	10	14

Table S3. Parameters obtained from the nitrogen desorption isotherm experiments.

Samples	BET surface area (m ² .g ⁻¹)	Pore volume (cm ³ g ⁻¹)	Pore size (Å)
Zn-TMU-5	548	0.265	17.71
Ni-Ti LDH	7.30	-	-
Zn-TMU-5@10%Ni-Ti LDH	386	0.227	16.12
Zn-TMU-5@30%Ni-Ti LDH	259	0.183	14.75
Zn-TMU-5@50%Ni-Ti LDH	187	0.146	13.49